HIGH-SPECTRAL RESOLUTION SOLAR MICROWAVE OBSERVATIONS

Gordon J. Hurford

Caltech, Pasadena, CA 91125

ABSTRACT

The application of high-spectral resolution microwave observations to the study of solar activity is discussed with particular emphasis on the frequency dependence of microwave emission from solar active regions. A "shell model" of gyroresonance emission from active regions is described which suggests that high-spectral resolution, spatially-resolved observations can provide quantitative information about the magnetic field distribution at the base of the corona. Corresponding observations of a single sunspot with the Owens Valley frequency-agile interferometer at 56 frequencies between 1.2 and 14 GHz are presented. The overall form of the observed size and brightness temperature spectra was consistent with expectations based on the shell model, although there were differences of potential physical significance. The merits and weaknesses of microwave spectroscopy as a technique for measuring magnetic fields in the solar corona are briefly discussed.

I. INTRODUCTION

During the past solar maximum, considerable insight into many aspects of solar activity has been gained through the use of high-spatial resolution microwave observations (e.g., Dulk, 1985; Kundu and Vlahos, 1982; Marsh and Hurford, 1982). The value of such observations has been not only to reveal the size, location, and morphology of the microwave sources but also to enable the brightness temperature of such sources to be determined. The brightness temperature, determined from the ratio of source flux to area, is the quantity which is related most directly to the physical conditions in the source or to the characteristics of the energetic particle population. For example, the brightness temperature of an optically thick, thermal plasma is equal to its electron temperature.

In this paper, we shall be concerned with the frequency dependence of microwave emission from active regions. Such emission can be divided into three frequency regimes depending on the location and physical mechanisms which dominate. In the first regime, at millimeter wavelengths, emission from the corona can be entirely neglected and the situation is dominated by thermal bremsstrahlung from the chromosphere. Active regions are relatively difficult to discern, except through absorption features associated with filaments (Figure 1).

At centimetric wavelengths, thermal bremsstrahlung from the corona begins to make a contribution to the observed surface brightness. The low density and high temperature of the corona can only provide a small optical depth, and so the resulting brightness temperatures fall well below coronal values. Gyroresonance opacity, however, can render the corona optically thick at locations where the magnetic field has the appropriate values. This is observed as small, localized areas in which the brightness temperature achieves coronal values.

At decimetric frequencies, the optical depth of thermal bremsstrahlung from the corona has increased to the point where coronal brightness temperatures can be approached so that the morphology of the corresponding microwave maps changes again (e.g., Dulk and Gary, 1983), almost to the point of being suggestive of soft X-ray maps.

For many active regions, observations at the VLA frequencies, 15, 5, and 1.4 GHz, would yield three different morphologies, corresponding to these three regimes.

This paper will be concerned with the frequency dependence of active region emission in the second regime where gyroresonance opacity is important. It will be suggested that the size and brightness temperature spectrum of the compact microwave sources can be used to directly measure the strength and distribution of coronal magnetic fields. This suggestion will be illustrated by preliminary results of high-spatial and high-spectral resolution, multifrequency observations of a solar active region.

II. A SHELL MODEL OF MICROWAVE EMISSION

Let us now consider in more detail some characteristics of the gyroresonance emission from active regions, with particular emphasis on what might be learned from the frequency dependence of such emission. To simplify the discussion, we consider the case of a single isolated sunspot. In the absence of gyroresonance opacity, thermal bremsstrahlung would yield emission with brightness temperatures of 10^4 to 10^5 K. Under the specific conditions where gyroresonance can be effective, however, the increased brightness temperature to $\sim 10^6$ K would be readily observable as a bright source against a relatively cool background. The corresponding sources have been observed by many workers with high-resolution, microwave imaging instruments such as the Very Large Array and the Westerbork Interferometer (e.g., McConnell and Kundu, 1984; Lang, Willson, and Gaizauskas, 1983).

Gyroresonance opacity is significant at frequencies which are low integral multiples of the local gyrofrequency, ν_g (GHz) = 2.8 B (kG). It is important to recall that the gyrofrequency depends only on the magnetic field, B, and is independent of electron temperature, density, or velocity. At temperatures and densities typical of coronal conditions, gyroresonance opacity usually provides significant optical depth at the 2nd and 3rd harmonics in the extraordinary propagation mode (left circular polarization for downward directed fields) and at the 2nd harmonic in the ordinary mode. The optical depth at higher harmonics is usually much less than 1 and so can be neglected.

These considerations lead to the schematic picture, illustrated in Figure 3, whereby at a fixed frequency, the coronal microwave emission above a sunspot is generated in magnetic shells, representing isogauss surfaces. At 5 GHz for example, the emission would come from shells where the magnetic fields are approximately 600 and 900 Gauss. (At 600 and 900 Gauss, the gyrofrequencies are 1.7 and 2.5 GHz, whose 2nd and 3rd harmonics are 5 GHz.) Thus, at 5 GHz, the ordinary mode emission comes from a surface where the magnetic field is 900 Gauss, whereas the extraordinary mode emission comes from a 600-Gauss shell. (In the extraordinary mode, the 900-Gauss shell also would emit at 5 GHz, but such emission normally would be hidden under the opaque 600-Gauss shell.)

To imaging observations, these shells appear as the localized areas with coronal brightness temperature. The diameter of the observed sources is determined by the intersection of the isogauss shells with the transition region. (Emission by the shell below the transition region is unimportant since even if it were optically thick, it could not have 10^6 K brightness temperature.) Thus, the outline of the resulting 10^6 K source represents a specific isogauss contour at the base of the corona.

In this picture, observations at a different frequency would correspond to a correspondingly different magnetic field contour. For example, at higher frequencies, the emission shells would correspond to stronger fields and a decreased source diameter would be expected. In fact, at a frequency corresponding to the shell which is tangent to the transition region, we would expect that the diameter would approach zero and that at frequencies above this cutoff, coronal brightness temperatures would not be achieved.

Note that the diameter of these shells as a function of frequency depends on the configuration of the magnetic field in the corona. Rapidly diverging fields would differ markedly from well constrained flux tubes in terms of the variation of the contour diameter with field at the base of the corona. Thus, measurement of the diameter and temperature of the corresponding microwave sources as a function of frequency could provide a direct, quantitative measurement of the magnetic field distribution at the base of the corona.

III. OBSERVATIONS

To explore the feasibility of such a technique for determining coronal fields, observations were conducted with the frequency-agile interferometer of the Owens Valley Radio Observatory (OVRO). This system (Hurford, Read, and Zirin, 1984) can observe at up to 86 frequencies between 1 and 18 GHz in both right and left circular polarization (RCP,LCP). With its capability of rapid switching among frequencies, detailed spectra can be obtained in a few seconds.

Early results (Hurford, Gary, and Garrett, 1985) used two antennas for measurements of active regions. With only a single baseline, it was not possible to directly measure the size of the sources. The resulting spectra were consistent, however, with the arguments advanced in Section I. Soviet workers (cf., Akhmedov et al., 1983) have conducted corresponding multifrequency measurements between 7.5 and 15 GHz using their RATAN-600 instrument.

The present results are based on the first such interferometric measurements using three antennas. At the time of these observations, the east-west separation of the antennas was 0.183, 1.067, and 1.250 km with the central antenna displaced 0.032 km north of the line joining the outer two. The resulting resolution (fringe spacing) was inversely proportional to frequency (5 arc s at 10 GHz), which was more than adequate to resolve the sources at each frequency. The limited field of view afforded by the use of large antennas (27 to 40 m diameter paraboloids) made it possible to restrict the field of view to a single active region (at all but the lowest frequencies).

Calibration of interferometer amplitudes as a function of polarization, baseline, and frequency was based on extended observations of 3C273 and 3C84. The resulting amplitudes are estimated to be known to about 10%, with a principal source of uncertainty being an imperfect knowledge of the calibrator spectra.

The preliminary results discussed below are based on data acquired in right and left circular polarization (RCP,LCP) at 56 frequencies between 1.2 and 14 GHz during ~20 min integrations on 3 successive mornings (26-28 July 1984).

Optical data showed that the target region (AR4549) was dominated by a progressively weakening, single sunspot. Therefore, we anticipated that only a single gyroresonance source

would be present. This hypothesis was tested by forming the closure phase* (Pearson and Readhead, 1984) at each frequency and polarization and rejecting data which were inconsistent with the single gyroresonance source. (Rejected data were primarily at the highest and lowest frequencies where emission by thermal bremsstrahlung was competitive.)

To determine the size of the source at each frequency/polarization, a Gaussian profile was assumed. In this case the dependence of amplitude, A [Jy], on projected baseline, L [km], for a Gaussian source of FWHM diameter, D [arc s], observed at frequency, ν [GHz] is given by:

$$A = A_o \, e^{-9.3 \times 10^{-4} \, (LD\nu)^2}$$

where A_o [Jy] is the limiting amplitude at L = 0, corresponding to an unresolved source. Thus, a plot of ln(A) versus L^2 should be a straight line whose slope yields the value of D, the source diameter. A typical plot of this type, shown in Figure 3, shows that the diameter can be measured to an accuracy of about 5%.

Having measured the diameter and A_o, the corresponding brightness temperature is given by the ratio of source flux to area, using the relation,

$$T_b = 3.5 \times 10^6 \, A_o \, (D\nu)^{-2} \quad .$$

The resulting size and brightness temperature spectra for 26 July 1984 are illustrated in Figure 4. Figure 5 shows the evolution of these quantities over the three successive days as the sunspot decayed.

IV. RESULTS

In broad terms, the features of the spectra in Figure 4 are consistent with expectations based on the shell model discussed in Section II. For example, in LCP (extraordinary mode emission) the brightness temperature maintained coronal values up to ~12 GHz while below this frequency the source size increased as frequency decreased. The interpretation is that the isogauss contours at the base of the corona are larger at the weaker fields corresponding to the lower frequencies. Above 12 GHz, the brightness temperature is seen to drop rapidly to a few times 10^5 K. This is consistent with the expectation that the brightness temperature would fall at a transition frequency where the corresponding isogauss shell was tangent to the transition region. The relatively constant value of source size above ~10 GHz is not understood at present, but might be related to spatial fragmentation of high frequency sources such as observed by Lang, Willson, and Gaizauskas (1983) at 15 GHz. (A group of unresolved sources would be seen by a three-element interferometer to have a diameter corresponding to their spatial envelope and a correspondingly diluted brightness temperature.)

Comparing the RCP and LCP brightness temperature spectra, we note that the same qualitative behavior is observed in RCP as in LCP. Of particular interest, however, is the fact that shifting the RCP spectrum up in frequency by a factor of 3/2 provides a reasonable agree-

*Closure phase can be defined an appropriately signed sum of the interferometer phases observed on the three baselines. Its usefulness here is derived from the fact that the closure phase should be zero for the expected small, single, symmetrical source, and generally nonzero for more complex sources.

ment with the LCP brightness temperature spectrum. This is consistent with the expectation that the 2nd and 3rd harmonics are the highest ones that are optically thick in the ordinary and extraordinary modes, respectively.

Some aspects of the spectra in Figure 4 are not understood at present. A scaled comparison of the RCP and LCP size spectra might be expected to behave in the same manner as the scaled brightness temperature spectra. Although they are indeed consistent in terms of the size and scaled frequency at which the size levels off, the RCP results at lower frequencies seem significantly higher than expected on the basis of the LCP spectra. Another unexpected feature is the apparent systematic increase from 2 to 4 x 10^6 K as frequency increases. The significance of this in terms of the physics of the coronal fields is not clear.

The evolution of the coronal field as the sunspot disappeared is illustrated in Figure 5. Assuming that the 3rd harmonic is the relevant one in the extraordinary mode, from the brightness temperature spectra, it is apparent that the maximum field at coronal levels decreased from about 1300 to 1000 to 600 G over a 2-day period. The relatively modest change in the size spectra at the lower frequencies over this period is also significant. It may suggest that the weaker fields were not affected by the spot's disappearance to the same extent as were the stronger fields.

Another interesting facet to the field evolution was the systematic decline in brightness temperature associated with the strongest fields on each day, from 4 to 2 to 1 x 10^6 K.

V. DISCUSSION

The observations presented above represent preliminary analyses of the first interferometric size and brightness temperature spectra of an active region. The region selected for this analysis was deliberately chosen to be a simple one, a single isolated sunspot. In broad terms, we have seen that the spectra matched expectations based on straightforward application of gyroresonance effects, as exemplified by magnetic shells. We have also seen that there are some aspects of the spectra that are not yet understood.

At this stage, it is perhaps premature to consider detailed interpretation of the data in terms of the solar coronal fields. Nevertheless, it may be worthwhile to comment on the strengths and weaknesses of microwave spectroscopy (as now understood) for the measurement of such fields.

Unlike photospheric magnetograms which measure magnetic FLUX (averaged over the seeing-dependent instrumental resolution), microwave spectroscopy depends on the magnetic FIELD in the corona. (Thus, for example, the present data are inconsistent with a model in which much of the coronal field is concentrated in small bundles of intense field.) Through the gyrofrequency, the field measurements are inherently calibrated. Thus, long-term comparisons are quite feasible. More complete exploitation of the interferometer phase data will enable the location of the coronal fields to be accurately established. In such circumstances, limb observations would enable the field profile as a function of height to be directly determined. Finally, since measurements such as these can be made in a few seconds, insight into flare-related coronal fields can be expected as well.

The use of microwave spectroscopy for the measurement of coronal fields has some clear weaknesses. As our model suggests, the magnetic measurements represent emission coming from a

range of heights, characterized by temperature, not distance above the photosphere. Thus, although the measured isogauss contours refer to the base of the corona, the corresponding temperature values average over a range of heights. There can also be potential sources of ambiguity related to the specification of the appropriate harmonic, particularly for magnetic fields directed close to the line of sight. This, however, can be overcome in a straightforward manner with more detailed calculation of the emission (e.g., Kruger, Hildebrandt, and Furstenberg, 1985; Hurford, Gary, and Garrett, 1985). Perhaps the most serious weakness, however, is that with a three-element interferometer, there are limitations as to the morphological complexity of active regions which can be effectively studied. This problem cannot be resolved without the addition of more antennas.

Despite these weaknesses, these preliminary results suggest that microwave spectroscopy has the potential to directly determine the magnetic field profile at the base of the corona. Given the importance of coronal fields to many aspects of solar activity, this may prove a useful adjunct to the next generation of coronal and hard X-ray imaging instrumentation.

Acknowledgments. Dr. D. E. Gary, Dan Briggs, Margaret Liggett, and Dan Daugherty have made important contributions to this work. Support for the solar observing program at Owens Valley is provided by the NSF under grants AST-8315217 and ATM-8309955 and by AFGL under contract F19628-84-K-0023.

REFERENCES

Akhmedov, Sh. B., Gelfreikh, G. B., Furstenberg, F., Hildebrandt, J., and Kruger, A., 1983, *Solar Phys., 88,* 103.

Dulk, G. A., 1985, these proceedings.

Dulk, G. A. and Gary, D. E., 1983, *Astron. Astrophys., 124,* 103.

Hurford, G. J., Read, R. B., and Zirin, H., 1984, *Solar Phys., 94,* 413.

Hurford, G. J., Gary, D. E., and Garrett, H. B., 1985, *Radio Stars* (R. M. Hjellming and D. M. Gibson, eds.), D. Reidel, p. 379.

Kruger, A., Hildebrandt, J., and Furstenberg, F., 1985, *Astron. Astrophys., 143,* 72.

Kundu, M. R. and Vlahos, L., 1982, *Space Sci. Rev., 32,* 405.

Lang, K. R., Willson, R. F., and Gaizauskas, V., 1983, *Astrophys. J., 267,* 455.

Marsh, K. A. and Hurford, G. J., 1982, *Ann. Rev. Astron. Astrophys., 20,* 497.

McConnell, D. and Kundu, M. R., 1984, *Astrophys. J., 279,* 421.

Pearson, T. J. and Readhead, A. C. S., 1984, *Ann. Rev. Astron. Astrophys., 22,* 97.

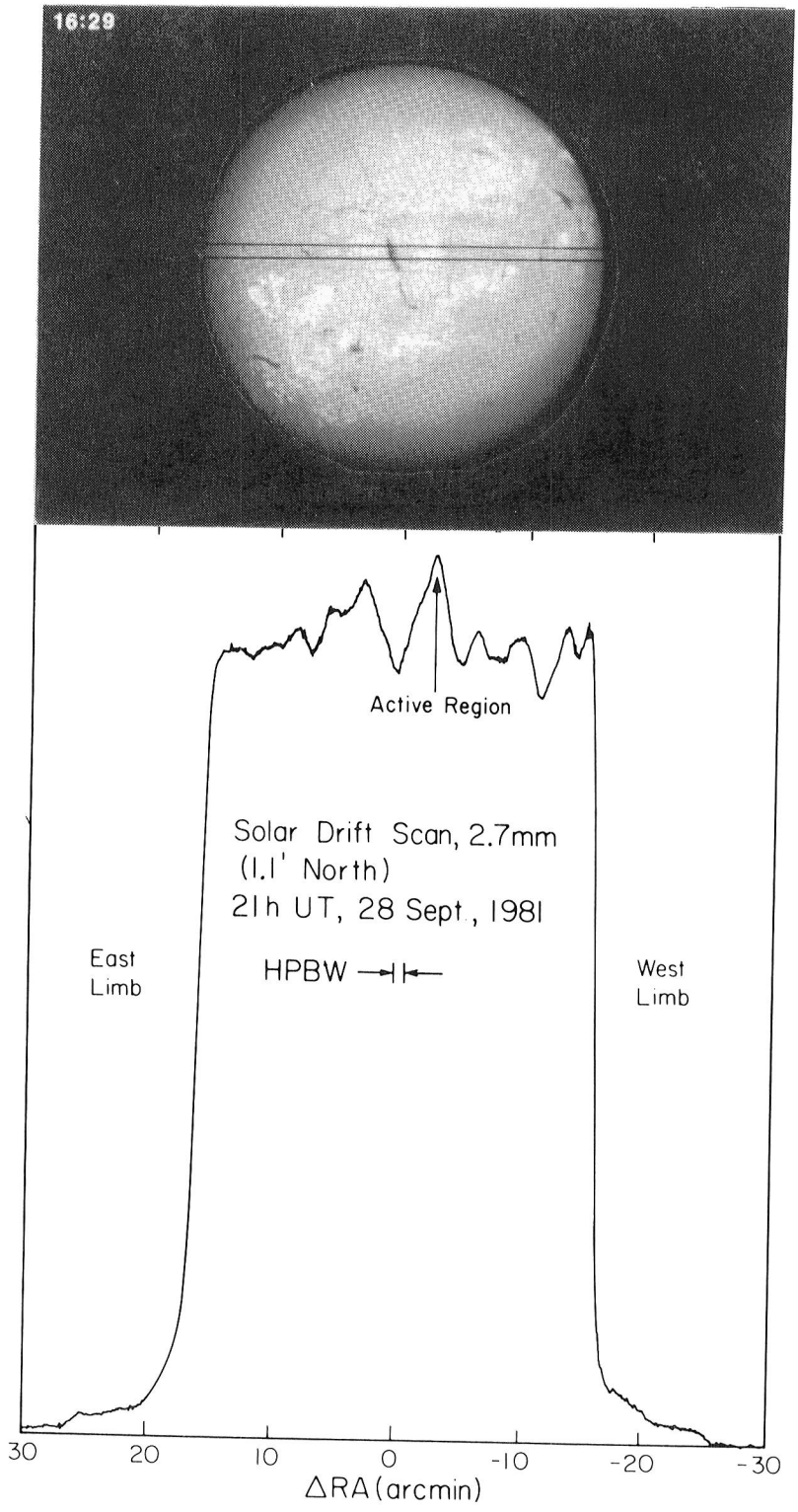

Figure 1. Comparison of a solar profile at 114 GHz with the corresponding Hα full-disk image. The two parallel lines on the optical image show the track of the half-power points of the radio beam as it scanned the Sun. Even when the beam crossed an active region, the brightness temperature did not significantly exceed its ~7000 K average value. The most striking correspondence is between the filaments in Hα and absorption features in the radio. (The data were acquired by a 10 m telescope at Owens Valley in collaboration with P. G. Wannier and G. A. Seielstad.)

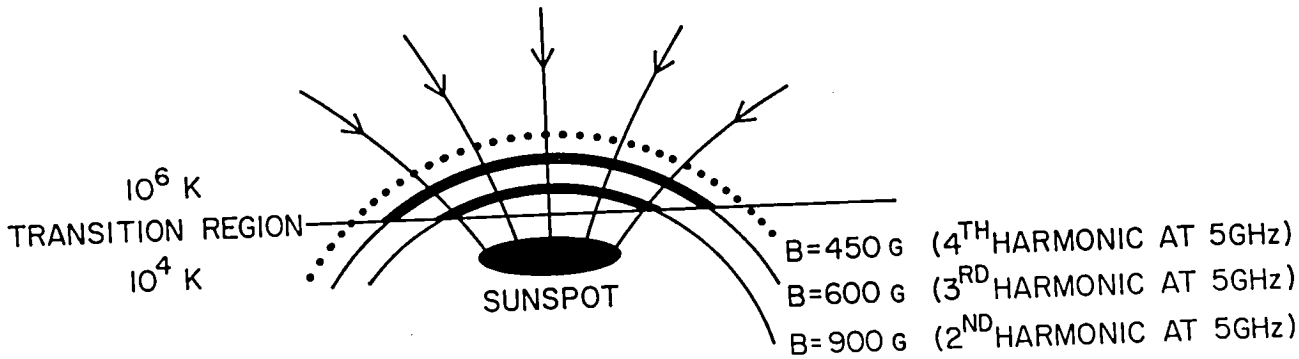

Figure 2. Schematic illustration of magnetic field lines above an isolated sunspot showing isogauss contours for 450, 600, and 900 Gauss.

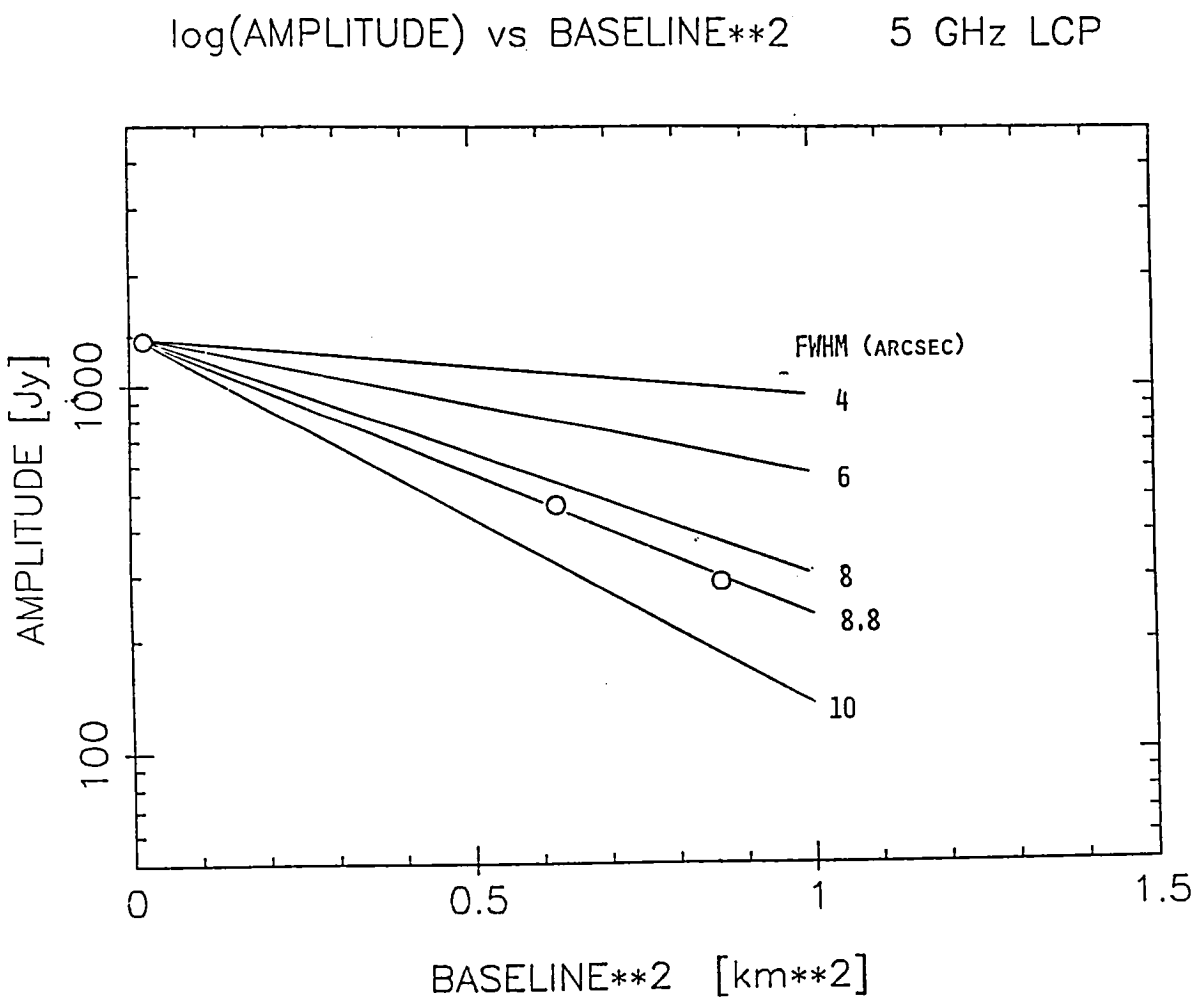

Figure 3. A typical plot showing the dependence of observed amplitude (circles) on projected baseline. Gaussian sources of different FWHM diameters would yield lines with the slopes as indicated. In this case the source FWHM diameter is 8.8 arc s.

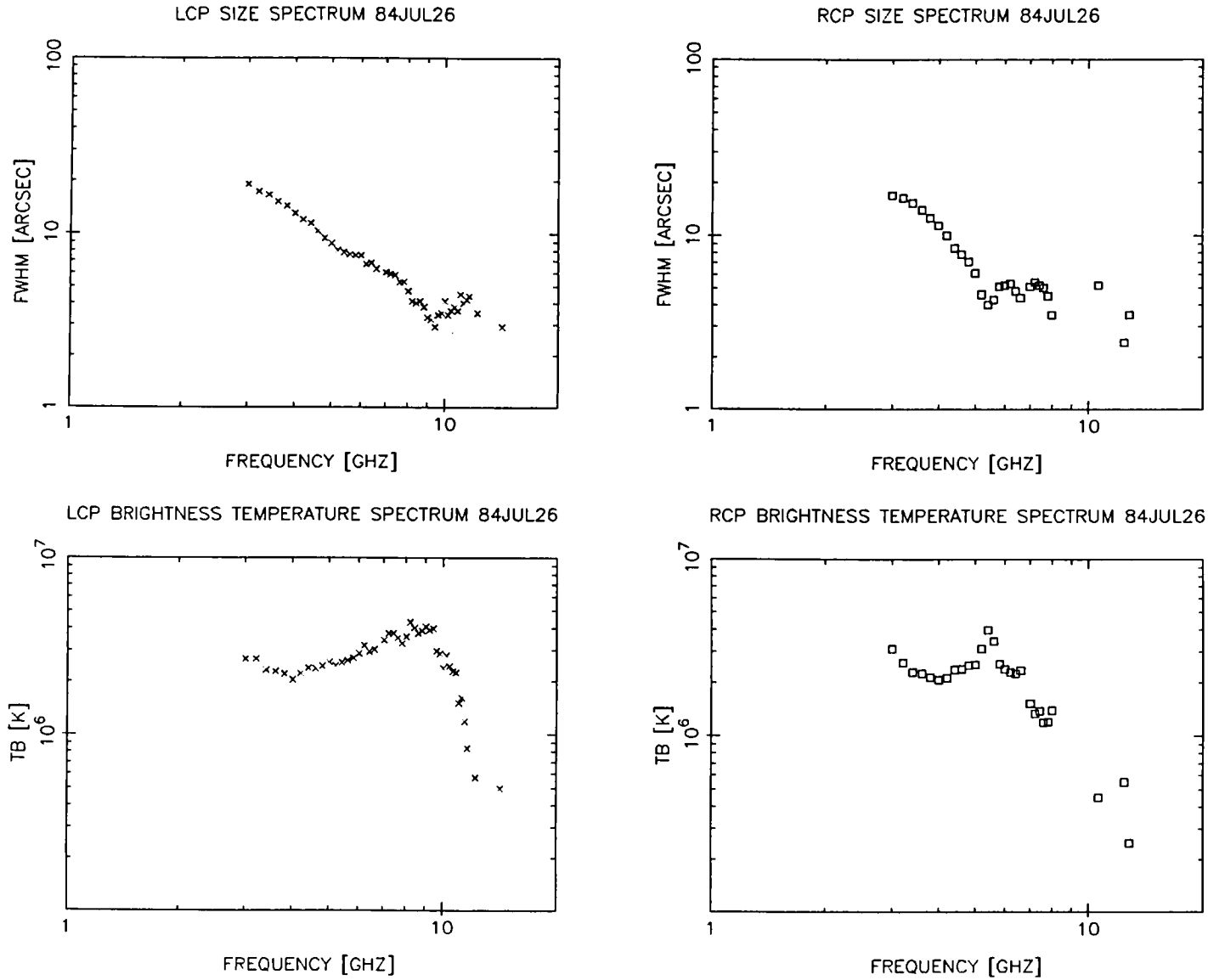

Figure 4. Size (top) and brightness temperature (bottom) spectra in LCP and RCP, respectively, as observed on 26 July 1984.

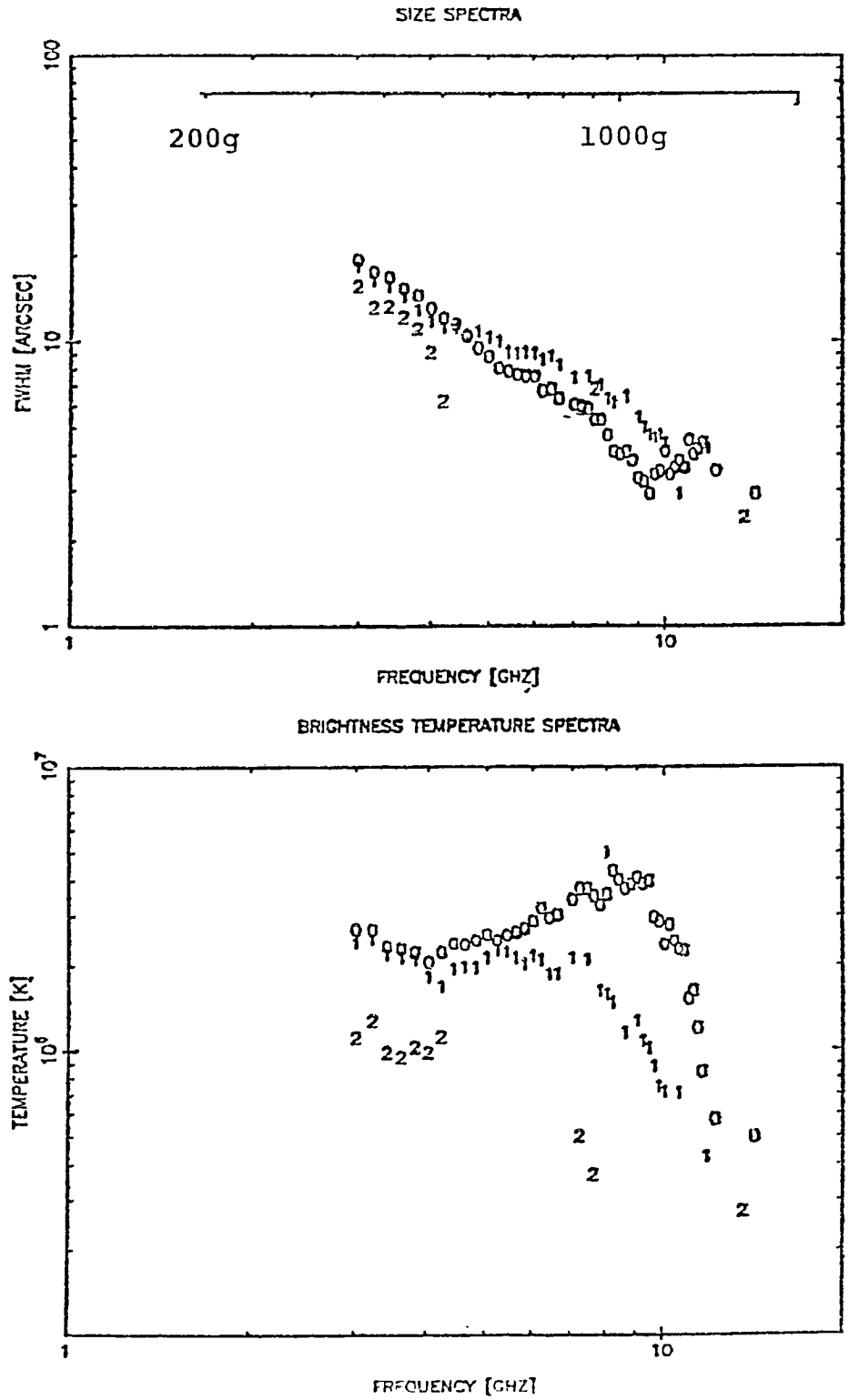

Figure 5. Evolution of the LCP (extraordinary mode) size (top) and brightness temperature (bottom) spectra as the sunspot disappeared. Data acquired on 26, 27, and 28 July are represented by 0, 1, and 2, respectively. With the assumption that the 3rd is the highest optically thick harmonic, the frequency scale can be interpreted in terms of the magnetic field scale inserted at the top.